

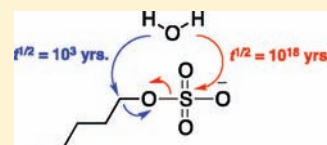
Catalytic Proficiency: The Extreme Case of S–O Cleaving Sulfatases

David R. Edwards,* Danielle C. Lohman, and Richard Wolfenden*

Department of Biochemistry and Biophysics, University of North Carolina, Chapel Hill, North Carolina 27599, United States

Supporting Information

ABSTRACT: As benchmarks for judging the catalytic power of sulfate monoesterases, we sought to determine the rates of spontaneous hydrolysis of unactivated alkyl sulfate monoesters by S–O bond cleavage. Neopentyl sulfate proved to be unsuitable for this purpose, since it was found to undergo hydrolysis by a C–O bond cleaving mechanism with rearrangement of its carbon skeleton. Instead, we examined the temperature dependence of the spontaneous hydrolyses of aryl sulfate monoesters, which proceed by S–O cleavage. Extrapolation of a Bronsted plot [$\log(k_{25}^N) = (-1.81 \pm 0.09) \text{p}K_a^{\text{LG}} + (3.6 \pm 0.7)$] based on the rate constants at 25 °C for hydrolysis of a series of sulfate monoesters to a $\text{p}K_a^{\text{LG}}$ value of 16.1, typical of an aliphatic alcohol, yields $k_{25}^N = 3 \times 10^{-26} \text{ s}^{-1}$. Comparison of that value with established k_{cat} values of bacterial sulfatases indicates that these enzymes produce rate enhancements ($k_{\text{cat}}/k_{\text{uncat}}$) of up to 2×10^{26} -fold for the hydrolysis of sulfate monoesters. These rate enhancements surpass by several orders of magnitude the $\sim 10^{21}$ -fold rate enhancements that are generated by phosphohydrolases, the most powerful biological catalysts previously known. The hydrolytic rates of phosphate and sulfate monoesters are compared directly, and the misleading impression that the two classes of ester are of similar reactivity is dispelled.



INTRODUCTION

Sulfuryl transfer is involved in regulating the binding affinity between receptor and ligand complexes, the control of hormone levels, detoxification, and other biological activities.^{1,2} Together, sulfotransferases and sulfatases control the state of sulfation of proteins, carbohydrates, lipids, and steroids.^{1,2} In addition to their involvement in these natural processes, organosulfate esters enter the environment as xenobiotics in household and industrial waste, mainly in the form of surfactants.³ It has been estimated that organosulfates contribute as much as 30% to the total organic mass found in atmospheric aerosols⁴ and that they constitute 50% of the total sulfur content in soil samples.⁵ An improved understanding of the susceptibility of organosulfate esters to hydrolysis is needed for the design of new surfactants with desirable properties,⁶ for the development of mechanism-based inhibitors of sulfatase/sulfotransferase enzymes in disease,⁷ and to broaden our appreciation of hydrolytic reaction mechanisms in general.

Sulfate monoesters react with nucleophiles in aqueous solution to generate products derived from either S–O bond cleavage⁸ or C–O bond cleavage.⁹ Most sulfatases catalyze the hydrolysis of bonds of this type by S–O bond cleavage.¹ The spontaneous or pH-neutral hydrolysis of sulfate monoesters by S–O bond cleavage is known to be slow at ordinary temperatures. Thus, 4-nitrophenyl sulfate (2d), which might be considered an activated ester based on the acidity of the product alcohol ($\text{p}K_a^{\text{LG}} = 7.14$), is hydrolyzed with a half-life of 45 years at 25 °C at pH values near neutrality.⁸ Rates of S–O cleavage of less activated sulfate monoesters, with leaving group $\text{p}K_a^{\text{LG}}$ values much greater than ~ 7 , do not appear to have been reported.¹⁰

In the work described here, we set out to determine the rates of spontaneous hydrolysis of simple unactivated alkyl sulfate

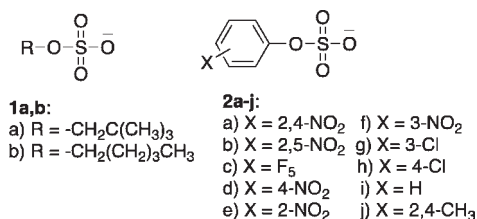


Figure 1. Chemical structures of sulfate monoesters 1 and 2.

monoesters by the S–O bond cleavage mechanism employed by sulfatases. Initially, we examined neopentyl sulfate (1a) as a model substrate, because the steric bulk of the neopentyl skeleton was expected to disfavor nucleophilic attack at carbon and because the absence of β -hydrogen atoms precludes the formal elimination of HSO_4^- (Figure 1). However, 1a was found to undergo hydrolysis by a C–O cleaving mechanism with rearrangement of its carbon skeleton. To circumvent that difficulty, we turned to the hydrolysis at elevated temperatures of sulfate esters of a series of aryl alcohols of progressively decreasing acidity, using the Eyring equation to estimate their reaction rates at ordinary temperatures. A Bronsted analysis of the results leads to the conclusion that hydrolysis of alkyl sulfate monoesters by S–O bond cleavage is an extraordinarily slow process and that the enzymes that promote these reactions are the most proficient biological catalysts identified to date. A kinetic rationale for the use of a formyl glycine nucleophile by aryl sulfatase enzymes is proposed.

Received: September 19, 2011

Published: November 16, 2011

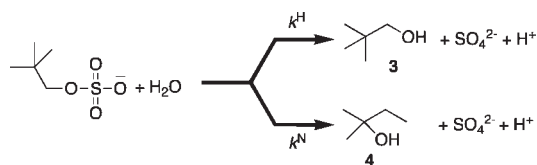


Figure 2. Hydrolysis of neopentyl sulfate (**1a**) forming a pH dependent mixture of **3** and **4**.

EXPERIMENTAL SECTION

Sulfate esters **1a,b** and **2c,f–j** were prepared by standard procedures as detailed in the Supporting Information. Other reagents were obtained from commercial sources and used as supplied. Deionized water (0.11 $\mu\text{S}/\text{cm}$) was used for all kinetic experiments.

Hydrolytic reactions were conducted in quartz tubes sealed under vacuum. The reaction vessels were placed in thermally equilibrated ovens equipped with ASTM thermometers for a set time period. Standard kinetic runs were carried out with 2.0×10^{-2} M sulfate monoester using 0.4 M of the described buffer system to maintain reaction pH. Typically the 0.2 mL reaction volume was divided into two portions. One portion was diluted 5-fold with H_2O and the pH measured using an Accumet standard glass combination electrode (Fisher Scientific). The second portion was diluted 5-fold with D_2O for ^1H NMR analysis run on an Inova 500 MHz spectrometer equipped with a 5 mm cold probe, using a 30 s delay between pulses. Reaction progress was determined by ^1H NMR for a given experiment at a single time point by comparison of the normalized integrated signal intensities corresponding to the starting material and reaction products. Observed first order rate constants were calculated using a standard first order exponential equation. First order behavior was verified by comparison of the computed rate constants determined at different time points for separate reactions run under otherwise identical conditions. Reactions were free of byproduct and obeyed good first order behavior for >90% conversion. $\text{p}K_a$ data for the aryl alcohol leaving groups of **2** were obtained from literature sources.¹¹ The $\text{p}K_a^{\text{LG}}$ for **1b** was estimated to be 16.1 using a σ^* of -0.13 by the method of Ballinger and Long.¹² ^{17}O NMR spectra were acquired on a 600 MHz Inova spectrometer operating at a frequency of 81.31 MHz using a 100 ms repetition rate.

RESULTS

A. Hydrolysis of Neopentyl Sulfate (1a). A 200 μL aqueous solution containing 2.0×10^{-2} M **1a** and 0.4 M formate buffer at pH 4.05 was sealed in a quartz tube under vacuum and heated to 180 $^\circ\text{C}$ for 110 min. Following reaction, the sealed quartz tube was cooled in an ice bath and the contents diluted 5-fold with D_2O for analysis by ^1H NMR using a standard water suppression sequence. ^1H NMR (500 MHz, D_2O) of the crude reaction mixture revealed the presence of unreacted **1a** and neopentanol (**3**) in a ratio of 82:18 as determined by comparison to authentic samples (Figure 2). An observed rate constant of $3.0 \times 10^{-5} \text{ s}^{-1}$ was calculated from the integrated signal intensities using a standard first order exponential equation. In a similar manner, **1a** was hydrolyzed at pH 7.6 maintained with potassium phosphate buffer (0.4 M) at 180 $^\circ\text{C}$ for 17.8 h. The ^1H NMR spectrum of this product mixture contained three new sets of peaks, corresponding to *tert*-amyl alcohol (**4**), in addition to unreacted **1a** (molar ratio of 1.1: 4.7). The observed rate constant for conversion of **1a** to **4** under these conditions was $3.3 \times 10^{-6} \text{ s}^{-1}$ (Figure 2).

B. pH Dependence of the Hydrolysis of 1a at 180 $^\circ\text{C}$. Rate constants for the disappearance of **1a**, forming a variable mixture

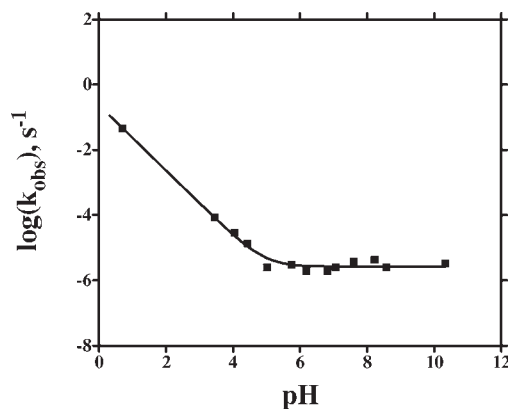


Figure 3. Plot of $\log(k_{\text{obs}})$ versus pH for the conversion of **1a** into a variable mixture of **3** and **4** at 180 $^\circ\text{C}$ as determined by ^1H NMR (500 MHz, D_2O). The kinetic constants $k^{\text{H}} = (2.3 \pm 0.4) \times 10^{-1} \text{ M}^{-1} \text{ s}^{-1}$ and $k^{\text{N}} = (2.7 \pm 0.3) \times 10^{-6} \text{ s}^{-1}$ were determined from a fit of the data to eq 1.

of **3** and **4**, were determined by ^1H NMR (500 MHz, D_2O) from pH 0.7–10.3 at 180 $^\circ\text{C}$ (Figure 3). In these experiments, pH was generally maintained constant over the course of the reaction with potassium formate, acetate or phosphate buffers (0.4 M).¹³ Control experiments using different concentrations of these buffer systems at constant pH showed small (<15%) effects on the computed observed rate constants. The hydrolysis of **1a** at pH 0.7 was too fast to measure at 180 $^\circ\text{C}$, and was estimated by extrapolation of an Eyring plot determined over the range $T = 60\text{--}130$ $^\circ\text{C}$ in the presence of 2.0×10^{-1} M HCl (vide infra). A fit of the kinetic data to eq 1 yielded $k^{\text{H}} = (2.3 \pm 0.4) \times 10^{-1} \text{ M}^{-1} \text{ s}^{-1}$ for the acid-catalyzed formation of **3** and $k^{\text{N}} = (2.7 \pm 0.3) \times 10^{-6} \text{ s}^{-1}$ for the neutral production of **4** (Figures 2 and 3). The ratio of rate constants for the neutral and acid catalyzed hydrolysis of **1a** is such that equal amounts of **3** and **4** are formed at the near neutral pH of 4.9.¹⁴

$$\log(k_{\text{obs}}) = \log(k^{\text{H}} \times 10^{-\text{pH}} + k^{\text{N}}) \quad (1)$$

C. Activation Parameters for the Hydrolysis of 1a and 1b.

Sulfate ester **1a** was hydrolyzed in the presence of potassium phosphate buffer (0.4 M, pH 8.1) over the temperature range spanning 160–243 $^\circ\text{C}$. Fitting the kinetic data to the Eyring equation yielded $\Delta H^\ddagger = 23.0 \pm 1.3 \text{ kcal/mol}$ and $\Delta S^\ddagger = -33 \pm 2.5 \text{ cal/mol}\cdot\text{K}$. Extrapolation of the Eyring plot led to an estimated rate constant of $5 \times 10^{-12} \text{ s}^{-1}$ at 25 $^\circ\text{C}$, corresponding to $t^{1/2} > 4000$ years for the neutral hydrolysis of **1a** (Table 1). Sulfate ester **1a** was also subjected to hydrolysis in 2.0×10^{-1} M HCl (pH 0.7) at temperatures ranging from 60 to 130 $^\circ\text{C}$, and second order rate constants were calculated as $k_2^{\text{H}} = k_{\text{obs}}/[\text{H}^+]$. The activation parameters $\Delta H^\ddagger = 31.5 \pm 0.05 \text{ kcal/mol}$ and $\Delta S^\ddagger = +7.3 \pm 0.1 \text{ cal/mol}\cdot\text{K}$ were determined by fitting the kinetic results to the Eyring equation. Extrapolation of the Eyring plot led to an observed first order rate constant of $1.9 \times 10^{-9} \text{ s}^{-1}$ ($t^{1/2} = \sim 12$ years) in 1 M HCl and 25 $^\circ\text{C}$. For comparison, *n*-pentyl sulfate (**1b**) was hydrolyzed from 94 to 185 $^\circ\text{C}$ in the presence of a 0.2 M ethyl phosphonic acid buffer at pH 7.4, where the hydrolysis of **1b** was independent of pH and buffer catalysis was found to be negligible. A fit of the rate data to the Eyring equation yields $\Delta H^\ddagger = 25.2 \pm 1.9 \text{ kcal/mol}$ and $\Delta S^\ddagger = -25 \pm 4 \text{ cal/mol}\cdot\text{K}$ for the pH neutral hydrolysis of **1b** (Table 1).

Table 1. Activation Parameters and Computed First Order Rate Constants, k_{25}^N , at 25 °C for the Neutral Hydrolysis of 1a, b and 2a–j

	pK_a^{LG}	ΔH^\ddagger (kcal/mol)	ΔS^\ddagger (cal/mol/K)	k_{25}^N (s^{-1}) ^a	$t_{25}^{1/2b}$
C–O bond cleavage					
1a	15.5 ^c	23.0 ± 1.3	−33 ± 2.5	5.0 × 10 ^{−12}	4.4 × 10 ³ yrs
1b	16.1	25.2 ± 1.9	−25 ± 4	6.8 × 10 ^{−12}	3.2 × 10 ³ yrs
S–O bond cleavage					
2a ^d	4.11	18.2	−18.0	(4.0 × 10 ^{−5}) ^d	6 h
2b ^d	5.04	18.8	−17.4	1.5 × 10 ^{−5}	13 h
2c	5.49	ND	ND	(9.9 × 10 ^{−8}) ^e	85 days
2d	7.14	25.9 ± 1.2	−16 ± 3	1.9 × 10 ^{−10}	45 yrs
2e ^d	7.21	24.1	−17.4	2.0 × 10 ^{−9}	11 yrs
2f	8.38	26.7 ± 1.3	−20 ± 4	6.7 × 10 ^{−12}	1.2 × 10 ³ yrs
2g	9.02	27.2 ± 0.9	−23 ± 2	6.3 × 10 ^{−13}	3.5 × 10 ⁴ yrs
2h	9.38	32.3 ± 1.9	−14 ± 4	1.3 × 10 ^{−14}	1.7 × 10 ⁶ yrs
2i	9.99	32.9 ± 1.0	−15 ± 2	2.3 × 10 ^{−15}	1.6 × 10 ⁷ yrs
2j	10.6	35 ± 5	−14 ± 9	1.1 × 10 ^{−16}	2.0 × 10 ⁸ yrs

^a k_{25}^N computed from the activation parameters listed in the table using the Eyring equation unless otherwise noted. ^b Calculated from k_{25}^N and a standard first order exponential equation. ^c The pK_a^{LG} for 1a has previously been assumed to be approximately 15.5 (ref 22), and we find this value to be sufficiently accurate for our limited purposes of providing a visual reactivity comparison in Figures 7 and Supporting Information Figure S11. ^d Data from ref 10. ^e k_{25}^N for 2c represents an observed first order rate constant determined by initial rates at pH 8.5 and 25 °C. Activation parameters were not determined for hydrolysis of this substrate. A standard error of ±5% was determined from duplicate runs.

D. ¹⁷O Labeling Experiments for Hydrolysis of 1a and 1b.

An isotope labeling experiment was conducted to identify the position of bond cleavage during the hydrolysis of 1a. A solution (0.05 M) of 1a at an initial pH of 2.85 (1.4 × 10^{−3} M HCl) was hydrolyzed at 150 °C in water containing 6.1 atom % excess ¹⁷O for 20 h, at which time the hydrolysis of 1a was >99% complete. After concentration to dryness at reduced pressure and reconstitution in D₂O to remove residual H₂¹⁷O,¹⁵ analysis by ¹⁷O NMR (81.4 MHz, D₂O) was carried out on a sample containing triethylammonium sulfate (0.015 M).¹⁶ The peak at 167 ppm shown in Figure 4a corresponds to ¹⁷O-sulfate, and by comparison to the intensity of the solvent peak we estimate 6.7% incorporation of the label. We interpret this result as consistent with quantitative incorporation of the ¹⁷O-label into SO₄^{2−} as would be expected for an S–O bond cleaving mechanism. In a similar manner, 1a was hydrolyzed at 200 °C and pH 8.4 (0.1 M phosphate) for >5 half-lives in water containing 6.1% H₂¹⁷O. The ¹⁷O NMR of the product mixture of this reaction showed a broad peak at 94 ppm determined to be the inorganic phosphate used as buffer in the reaction, but no peak corresponding to inorganic sulfate could be detected (Figure 4b). We estimate the lower limit of detection using this method as 1 × 10^{−4} M, indicating that at least 90% of the pH neutral hydrolysis of 1a occurs by C–O bond fission. Hydrolysis of 1b at pH 8.4 and 200 °C for 20 h led to identical results, consistent with a C–O bond cleavage of this substrate as well.

E. Hydrolysis of Aryl Sulfate Monoesters. Aryl sulfate monoesters 2d,f–j were hydrolyzed at elevated temperatures,

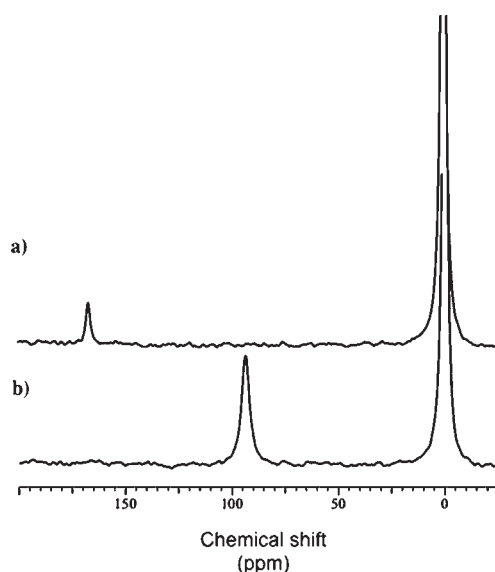


Figure 4. ¹⁷O NMR (81.4 MHz, D₂O) spectra of (a) recovered sulfate following the acid catalyzed hydrolysis of 1a at 150 °C where the peak at 167 ppm corresponds to ¹⁷O-sulfate and; (b) recovered sulfate following hydrolysis of 1a at pH 8.4 (0.1 M phosphate buffer), 200 °C where the peak at 94 ppm corresponds to ¹⁷O-phosphate. The spectra are referenced to D₂O at 0 ppm. The spectra in (a) and (b) were acquired with 256 and 1024 scans, respectively.

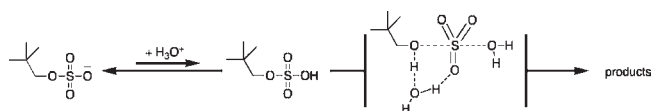


Figure 5. Proposed reaction mechanism for the acid catalyzed hydrolysis of 1a.

pH 8.4 (Supporting Information). Under these conditions, the hydrolytic reactions were shown to be independent of hydronium ion concentration and free of observable buffer effects. Activation parameters for the pH neutral hydrolysis of 2d,f–j were determined by fitting the rate data to the Eyring equation and are shown in Table 1 along with results for 2a, 2b, and 2e obtained from various sources.^{8,10} The activation parameters previously reported for the hydrolysis of 2d are $\Delta H^\ddagger = 24.4$ kcal/mol ($\Delta S^\ddagger = -19.5$ cal/mol/K) and $\Delta H^\ddagger = 24.6$ kcal/mol ($\Delta S^\ddagger = -18.5$ cal/mol/K) in satisfactory agreement with those determined here.^{8,17} Rate data for 2c were obtained at 25 °C and pH 8.4 by the method of initial rates, using UV spectrophotometry to monitor the release of pentafluorophenoxide at 260 nm (effective $\epsilon^{260} = 1023$).

DISCUSSION

A. Acid Catalyzed Hydrolysis of 1a. A mechanism consistent with the available data for the acid catalyzed hydrolysis of 1a is shown in Figure 5 involving a pre-equilibrium proton transfer from solvent to a nonbridging oxygen atom of the sulfate monoester. The pK_a of 1a can be estimated as −3.4,¹⁸ so the equilibrium shown in Figure 7 is expected to lie heavily toward the anionic sulfate monoester under the pH conditions of the current study. Heavy atom kinetic isotope effects on the acid catalyzed hydrolysis of 4-nitrophenyl sulfate support the transfer

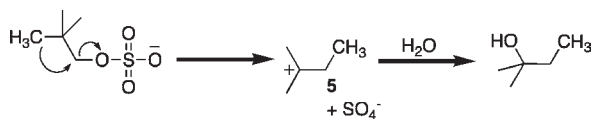


Figure 6. Proposed reaction mechanism for pH neutral hydrolysis of **1a** to form *tert*-amyl alcohol.

of the S–OH proton to the leaving group through a network of one or more water molecules concerted with S–O bond cleavage.¹⁷ It seems reasonable to suppose that a similar network of solvent molecules acts on alkyl sulfate **1a**, but there is evidence that the steric bulk of the neopentyl substituent may also disrupt the solvent shell surrounding the activated complex for reaction of this substrate. First, a Brønsted plot of the second order rate constants for the acid catalyzed hydrolysis of 5 aryl and 2 primary alkyl sulfate monoesters at 25 °C (Figure S11, Supporting Information)^{9,10,19} fits the equation:

$$\log(k_2^H) = (-0.33 \pm 0.01)pK_a^{LG} - (2.5 \pm 0.1)$$

Significantly, the point corresponding to **1a** lies approximately one logarithmic unit below the best fit line. Second, the entropy of activation for the acid catalyzed hydrolysis of the same five aryl and two alkyl sulfate monoesters is effectively substrate-independent, with an average ΔS^\ddagger of -3.4 ± 3 cal/mol/K, whereas ΔS^\ddagger for the acid catalyzed hydrolysis **1a** is distinctly more positive ($+7.3 \pm 0.2$ cal/mol/K). The acid catalyzed hydrolysis of **1a** is slower than expected relative to a suitable comparison provided by the Brønsted correlation and also involves a small but significantly increased activation entropy compared with the reactions of the other sulfate monoesters. These two observations would seem understandable if the large neopentyl substituent disrupted interactions with the surrounding solvent shell that would otherwise stabilize the activated complex through proton transfer relays and other polar interactions.

B. Spontaneous Hydrolysis of 1a/1b. The pH-independent hydrolysis of **1a** does not conform to the typical reaction mechanisms observed for sulfate monoesters, as evidenced by the rearrangement of the neopentyl carbon skeleton to form *tert*-amyl alcohol (**4**). The results of the ¹⁷O labeling study support a C–O bond cleaving mechanism such as the one presented in Figure 6, involving rate-limiting methyl migration with expulsion of SO_4^{2-} . Subsequent capture of cationic intermediate **5** by water or possibly hydroxide ion would then afford **4**. The sterically demanding neopentyl system has been known for some time to undergo solvolysis with rearrangement similar to that observed here, but the leaving groups have typically been highly reactive sulfonates.²⁰ We were therefore surprised to find that **1a**, equipped with a formally dianionic leaving group with $pK_a^{LG} = 1.8$,¹⁹ also underwent this process. Hydrolysis of the monoanionic 3-(4-carboxyphenyl)-2,2-dimethylpropyl phosphate monoester has been shown to generate the P–O bond cleavage product cleanly, without formation of detectable amounts of isomerized product.²¹ In a similar manner, the neutral hydrolyses of the monoanionic diesters bis-neopentyl phosphate and bis-(3-(4-carboxyphenyl)-2,2-dimethylpropyl) phosphate yield only P–O bond cleavage products.²² The observation that **1a** preferentially undergoes unimolecular rearrangement with elimination of SO_4^{2-} , rather than hydrolysis by S–O bond rupture, is consistent with the extreme inertness of this functional group to the latter mode of cleavage.²³

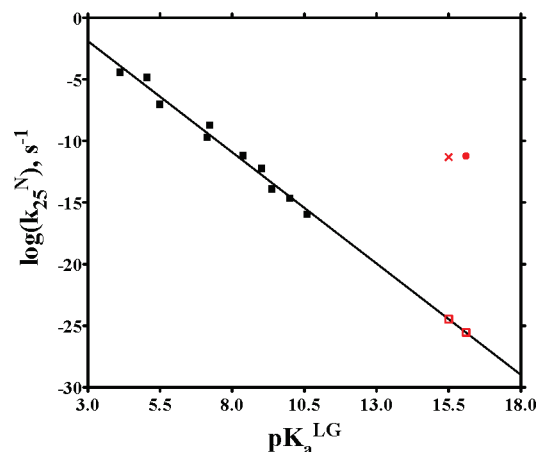


Figure 7. Brønsted plot of $\log(k_{25}^N)$ versus pK_a^{LG} for the hydrolysis of sulfate monoesters **2a–j** (■) at 25 °C fit to a standard linear regression of $\log(k_{25}^N) = (-1.81 \pm 0.09) pK_a^{LG} + (3.6 \pm 0.7)$, $r^2 = 0.9801$ (10 data). The experimental data for the neutral hydrolysis of **1a** (red cross) and **1b** (red solid circle) are shown for comparison along with the predicted rate constants for hydrolysis proceeding through S–O bond cleavage (open red square). The latter two data points are computed from the linear regression and have not been included in the fit.

Earlier experiments in this laboratory⁹ showed that a broad range of nucleophiles ($1.72 \leq pK_a^{Nu} \leq 15.7$) are alkylated by methyl sulfate in aqueous solution, furnishing a precedent for attack by weak nucleophiles, such as water, on alkyl sulfate monoesters. In fact methyl sulfate was found to be some 100-fold more reactive in this regard than the trimethylsulfonium ion. Consistent with these findings, **1b** undergoes spontaneous hydrolysis in the pH range 6–8 by attack of water on carbon to displace SO_4^{2-} .

C. Spontaneous Hydrolysis of Aryl Sulfate Monoesters. Rate constants, k_{25}^N , for the reaction of **2** at 25 °C can be calculated using the activation parameters in Table 1.²⁴ Notably, these are seen to vary by a factor of more than 10^{11} from the most reactive substrate (**2a**) to the least reactive (**2j**). The variation in reactivity of **2a–j** arises from the steep dependence of ΔH^\ddagger on the ionization constants, pK_a^{LG} , of the conjugate acids of the aryloxy leaving groups.²⁵ The ΔS^\ddagger values all fall within the relatively narrow range of -17 ± 3 cal/mol/K.

A Brønsted plot of $\log(k_{25}^N)$ versus pK_a^{LG} for hydrolysis of **2a–j** fits a standard linear regression of $\log(k_{25}^N) = (-1.81 \pm 0.09) pK_a^{LG} + (3.6 \pm 0.7)$ with a Brønsted coefficient of $\beta^{LG} = -1.8$ (Figure 7).²⁶ The β^{LG} determined here for hydrolysis of aryl sulfate monoesters at 25 °C is significantly more negative than that reported for the hydrolysis of a limited set of nitrophenyl and dinitrophenyl sulfate monoesters at 100 °C, where $\beta^{LG} = -1.2$.¹⁰ This discrepancy originates in the steep dependence of ΔH^\ddagger on pK_a^{LG} for the neutral hydrolysis of aryl sulfate monoesters. A decrease in reaction temperature results in the rates of hydrolysis for the less activated substrates being disproportionately reduced relative to the rates of hydrolysis of the more activated sulfate esters. The result is a gradual increase in the steepness of the observed Brønsted plot with decreasing temperature.

The equilibrium Brønsted coefficient, β^{eq} , determined for the transfer of the sulfonyl group between oxyanion nucleophiles at 25 °C is -1.74 .²⁷ Accordingly, the large negative β^{LG} of -1.8 observed here indicates that the leaving groups in **2a–j** have undergone near complete bond cleavage and bear formal charges

of approximately -1 at the transition state for hydrolysis. It might be suggested on this basis that hydrolysis of aryl sulfate monoesters proceeds via a fully dissociative $D_N + A_N$ mechanism. However, the Brønsted coefficient, β^{LG} , reports solely on the extent of bond cleavage to the leaving group and therefore cannot be used to distinguish a $D_N + A_N$ mechanism from an dissociative $A_N D_N$ process involving little bond formation to a nucleophilic water molecule. Based on heavy atom kinetic isotope effects, Hengge et al. have described the hydrolysis of 4-nitrophenyl sulfate as involving an "exploded" transition state structure in which the sulfur trioxide moiety is only minimally bonded to the incoming water nucleophile and the departing aryloxy. ¹⁷ The linear free energy results presented here support this view, and, in fact, there is a remarkable agreement regarding the extent of charge development on the leaving group in the transition state arising from the two studies. A charge map for the spontaneous hydrolysis of aryl sulfate monoesters is shown in Figure 8 displaying the formal charge born by the aryloxy group in the ground, transition and product states.

D. Catalytic Proficiency and Rate Enhancements Provided by Sulfatase Enzymes. Earlier, a rate enhancement (k_{cat}/k_{uncat}) of at least 10^{11} was estimated for sulfatases, based on the rate of spontaneous methyl sulfate hydrolysis, without reference to the site of bond cleavage. ⁹ We are now in a position to offer a more concrete estimate of the effectiveness of sulfatases that catalyze S–O bond cleavage (Table 2). An alkylsulfatase from the bacterium coryneform B1a catalyzes the hydrolysis of linear alkyl sulfates by S–O bond cleavage. ²⁸ The reported kinetic parameters for the enzymatic hydrolysis of **1b** are $k_{cat} = 6.9 \text{ s}^{-1}$ and $k_{cat}/K_m = 3.6 \times 10^3 \text{ M}^{-1} \text{ s}^{-1}$ at pH 7.5. Rate constants for the spontaneous hydrolysis of **1b** by S–O bond cleavage are not directly accessible by experiment. However, a first order rate constant of $3 \times 10^{-26} \text{ s}^{-1}$ can be estimated by extrapolation of the Brønsted plot in Figure 7 to a pK_a^{LG} of 16.1 corresponding to *n*-pentanol under the reasonable assumption that the correlation obtains for both alkyl and aryl sulfate esters. ²⁹ An enzymatic

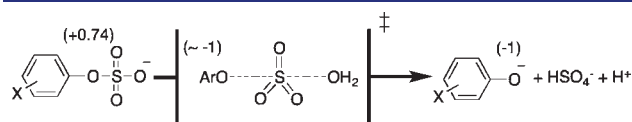


Figure 8. Charge map for the pH neutral hydrolysis of aryl sulfate esters **2a–j** where formal charges on the aryloxy leaving group are indicated in parentheses.

rate enhancement (k_{cat}/k_{non}) of 2×10^{26} -fold, or a catalytic proficiency ($(k_{cat}/K_m)/k_{uncat}$) of $1 \times 10^{29} \text{ M}^{-1}$ are calculated. Another S–O bond cleaving sulfatase, the D-lactate-2-sulfatase (EC 3.1.6.17) from *Pseudomonas syringae* GG, catalyzes the hydrolysis of its preferred substrate with $k_{cat} = 13.1 \text{ s}^{-1}$ and $k_{cat}/K_m = 2.0 \times 10^3 \text{ M}^{-1} \text{ s}^{-1}$. ³⁰ Extrapolation of the Brønsted plot in Figure 7 to a pK_a^{LG} of 15.1 ³¹ indicates a first order rate constant of $2.0 \times 10^{-24} \text{ s}^{-1}$ for the spontaneous hydrolysis of lactate-2-sulfate. A rate enhancement of $k_{cat}/k_{uncat} = 7 \times 10^{24}$ -fold and a catalytic proficiency of $(k_{cat}/K_m)/k_{uncat} = 1 \times 10^{27} \text{ M}^{-1}$ are calculated. A third example, the *Pseudomonas aeruginosa* arylsulfatase generates a 2.3×10^{10} -fold rate enhancement for the hydrolysis of **2d**, with a catalytic proficiency of $1 \times 10^{17} \text{ M}^{-1}$. ³²

Most sulfatases have been reported to catalyze the selective hydrolysis of sulfate monoesters by S–O bond fission, ¹ but a few prokaryotic sulfatases have been shown to catalyze C–O bond cleavage of alkyl sulfate monoesters. For example, the P2 primary alkylsulfohydrolase from *Pseudomonas* C12B catalyzes the hydrolysis of **1b** at an optimal pH of 8.3 (30 °C) with $k_{cat}/K_m = 320 \text{ M}^{-1} \text{ s}^{-1}$ by what is almost certainly a C–O bond cleaving mechanism. ³³ That value indicates a rate enhancement (k_{cat}/k_{uncat}) of 7×10^{11} and a catalytic proficiency ($(k_{cat}/K_m)/k_{uncat}$) of $3 \times 10^{13} \text{ M}^{-1}$ (Table 2).

E. Comparing the Rates of Hydrolysis for Phosphate and Sulfate Monoesters. Alkaline phosphatase catalyzes the hydrolysis of phosphate monoester dianions via a two-step ping-pong mechanism involving the formation of a phosphoserine intermediate (eq 2). ³⁴ Aryl sulfatases employ a variation on this mechanism to hydrolyze sulfate monoesters. In this case, the active site nucleophile is identified to be a formyl glycine (fGly) residue, which releases inorganic sulfate by C–O bond cleavage in the second step of the reaction (eq 3). ³⁵ We rationalize the different catalytic mechanisms employed by the enzymes by considering the relative rates of hydrolysis for alkyl phosphate versus alkyl sulfate monoesters.

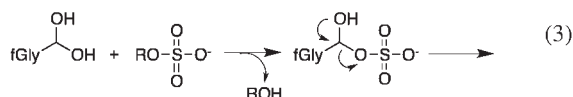
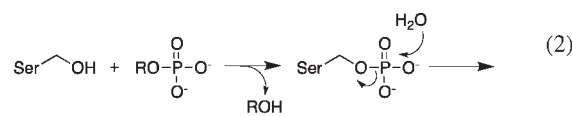


Table 2. Rate Enhancements and Catalytic Proficiencies of Sulfatases and Phosphatases^a

	$k_{cat} \text{ (s}^{-1}\text{)}$	$k_{cat}/K_m \text{ (M}^{-1} \text{ s}^{-1}\text{)}$	$k_{uncat} \text{ (s}^{-1}\text{)}$	catalytic proficiency $(k_{cat}/K_m)/k_{uncat} \text{ (M}^{-1}\text{)}$	rate enhancement k_{cat}/k_{uncat}
sulfatases					
P2 primary alkylsulfohydrolase ^b	9.7	321	1.4×10^{-11}	3×10^{13}	7×10^{11}
arylsulfatase	14.2	4.9×10^7	4.9×10^{-10}	1×10^{17}	3×10^{10}
D-lactate-2-sulfatase	13.1	2.0×10^3	2×10^{-24}	1×10^{27}	7×10^{24}
alkylsulfatase	6.9	3.6×10^3	3×10^{-26}	1×10^{29}	2×10^{26}
phosphatases					
inositol 1-phosphatase	22	3×10^5	$(2 \times 10^{-20})^c$	2×10^{25}	1×10^{21}
fructose bisphosphatase	21	1.5×10^7	$(2 \times 10^{-20})^c$	8×10^{26}	1×10^{21}
protein phosphatase 1	39	4×10^6	$(2 \times 10^{-20})^c$	2×10^{26}	2×10^{21}

^aData correspond to S–O (or P–O) bond cleavage unless specified otherwise. ^bC–O bond cleavage. ^cData from ref 21.

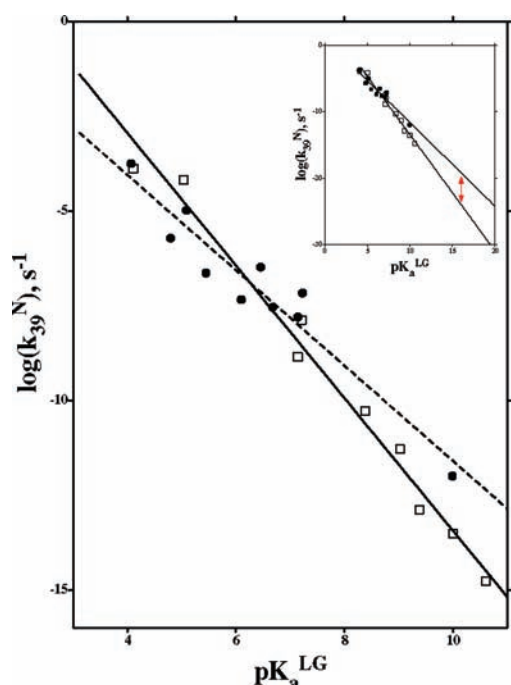


Figure 9. Brønsted plot of $\log(k_{39}^N)$ versus pK_a^{LG} for the hydrolysis of sulfate monoesters **2a–j** (\square) and aryl phosphate monoester dianions³⁸ (\bullet) at 39 °C. Inset: Horizontal axis has been extended so that the predicted reactivities of alkyl phosphate and sulfate monoesters can be compared.

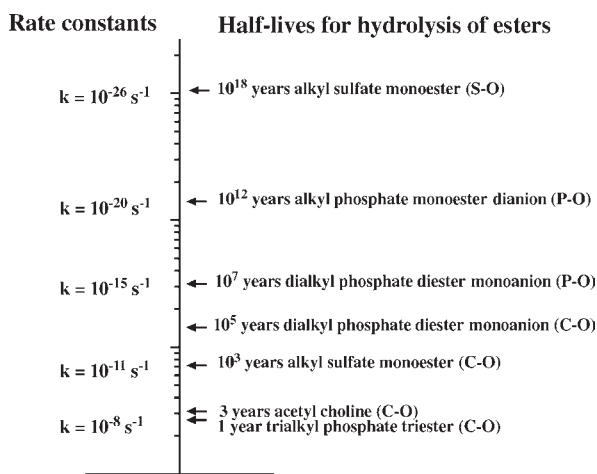


Figure 10. Half-lives for the hydrolysis of sulfo-, phospho-, and carbonyl esters at 25 °C.

At 39 °C, the activated substrates 2,4-dinitrophenyl phosphate (dianion) and 2,4-dinitrophenyl sulfate are hydrolyzed with very similar rate constants of 1.8×10^{-4} and $1.3 \times 10^{-4} \text{ s}^{-1}$, respectively.³⁶ On the other hand, the rate constant for hydrolysis of **1b**, an unactivated sulfate monoester, is estimated to be $7 \times 10^{-25} \text{ s}^{-1}$ at this same temperature. This value is approximately 5 orders of magnitude slower than that estimated for the corresponding alkyl phosphate monoester where a rate constant of $5 \times 10^{-20} \text{ s}^{-1}$ is indicated.³⁷ A side-by-side reactivity comparison of a series of phosphate and sulfate monoesters at 39 °C is presented in Figure 9.³⁸ The gradient of the line corresponding

to reaction of the sulfate monoesters is significantly steeper ($\beta^{LG} = -1.75$) than that for the phosphate monoester dianions ($\beta^{LG} = -1.26$). The net result, clearly apparent in the Figure, is a divergence in reactivity for phosphate and sulfate monoesters as the leaving group becomes less activated (higher pK_a^{LG}). The inset of Figure 9 shows the $\sim 10^5$ fold difference in reactivity expected for hydrolysis of alkyl phosphate and sulfate monoesters. We propose that this difference in reactivity compels the aryl sulfatase to seek an alternate mechanism, such as the one presented in eq 3, to circumvent the difficult task of cleaving an alkyl sulfo-enzyme intermediate by S–O bond cleavage.

CONCLUSION

The totem in Figure 10 displays the rate constants (and half-lives) for the spontaneous hydrolysis of several classes of ester. The stability of alkyl sulfate monoesters toward hydrolysis exceeds that of phosphate monoesters by several orders of magnitude. The enzymes that catalyze hydrolysis of alkyl sulfate monoesters by S–O bond cleavage appear to be the most proficient enzymes identified to date providing catalytic rate enhancements of up to 10^{26} -fold. This value surpasses by several orders of magnitude the $\sim 10^{21}$ -fold rate enhancements that are generated by phosphohydrolases, the most powerful biological catalysts previously known (see Table 2 for a comparison of catalytic proficiency and rate enhancement provided by sulfatases and phosphatase).

ASSOCIATED CONTENT

S Supporting Information. Description of synthetic procedures and analytical data for **1a,b** and **2c,f–j**. Plot of $\log(k_2^H)$ versus pK_a^{LG} . Plot of $\log(k_2^N)$ versus pK_a^{LG} for the pH neutral hydrolysis of **2a,c,d**. Eyring plots for the hydrolysis of **1a,b** and **2d,f–j**. This material is available free of charge via the Internet at <http://pubs.acs.org>.

AUTHOR INFORMATION

Corresponding Author

richard_wolfenden@med.unc.edu; dredward@email.unc.edu

ACKNOWLEDGMENT

We thank Greg Young, Facility Manager for the UNC Biomolecular NMR laboratory Core Facility, for providing the ^{17}O NMR spectra. This work was supported by National Institutes of Health Grant GM-18325.

REFERENCES

- (1) Hanson, S.; Best, M.; Wong, C.-H. *Angew. Chem., Int. Ed.* **2004**, *43*, 5736.
- (2) Chapman, E.; Best, M.; Hanson, S.; Wong, C.-H. *Angew. Chem., Int. Ed.* **2004**, *43*, 3526.
- (3) Scott, M.; Jones, M. *Biochim. Biophys. Acta* **2000**, *1508*, 235.
- (4) Surratt, J. D.; Gomez-Gonzalez, Y.; Chan, A. W. H.; Vermeylen, R.; Shahgholi, M.; Kleindienst, T. E.; Edney, E. O.; Offenberg, J. H.; Lewandowski, M.; Jaoui, M.; Maenhaut, W.; Claeys, Flagan, R. C.; Seinfeld, J. H. *J. Phys. Chem. A* **2008**, *112*, 8345.
- (5) Kertesz, M.; Cook, A.; Leisinger, T. *FEMS Microbiol. Rev.* **1994**, *15*, 195.
- (6) Li, M.; Powell, M.; Razunguzwa, T.; O'Doherty, G. *J. Org. Chem.* **2010**, *75*, 6149.
- (7) Day, J. M.; Purohit, A.; Tutill, H. J.; Foster, P. A.; Woo, L. W.; Potter, B. V.; Reed, M. J. *Ann. N.Y. Acad. Sci.* **2009**, *1155*, 80.

- (8) Benkovic, S.; Benkovic, P. *J. Am. Chem. Soc.* **1966**, *88*, 5504.
- (9) Wolfenden, R.; Yuan, Y. *Proc. Natl. Acad. Sci. U.S.A.* **2007**, *104*, 83.
- (10) Fendler, E.; Fendler, J. *J. Org. Chem.* **1968**, *33*, 3852.
- (11) Ba-Saif, S.; Waring, M.; Williams, A. *J. Chem. Soc., Perkin Trans. 2* **1991**, 1653–1659.
- (12) Ballinger, P.; Long, F. *J. Am. Chem. Soc.* **1960**, *82*, 795.
- (13) The pH rate profile shown in Figure 3 was constructed at a reaction temperature of 453 K (180 °C) and the autoprotolysis constant, $K_{453\text{ K}}^w$, at this temperature can be arrived at in the following manner. The acidity constant, K_a , for the ionization of water ($\text{H}_2\text{O} \rightleftharpoons \text{H}^+ + \text{OH}^-$) is defined by the thermodynamic parameters $\Delta H = 13.5$ kcal/mol and $\Delta S = -27$ cal/mol/K, and from this we compute $K_a = 3.8 \times 10^{-13}$ at 453 K. It follows that $K_{453\text{ K}}^w = K_a \times [\text{H}_2\text{O}] = 3.8 \times 10^{-13} \times 55\text{ M} = 2.1 \times 10^{-11}$ under the assumption that the concentration of water is invariant with respect to temperature. The datum in Figure 3 corresponding to pH 10.3 was obtained in the presence of 450 mM KOH, where $\text{pH} = -\log(K_{453\text{ K}}^w / [\text{OH}^-])$. Thermodynamic data obtained from: Eisenberg, D.; Kauzmann, W. *The Structure and Properties of Water*; Oxford University Press: London, 1969.
- (14) Neutral pH at 453 K is computed to be ~ 5.3 where $K_{453\text{ K}}^w = [\text{H}^+][\text{OH}^-] = (10^{-5.3}) \times (10^{-5.3})$.
- (15) During this procedure, the organic reaction product neopentanol (**3**) is also removed (BP 113–114 °C).
- (16) Marker, A.; Roy, A. *Biochim. Biophys. Acta* **1983**, *742*, 446.
- (17) Hoff, R.; Larsen, P.; Hengge, A. *J. Am. Chem. Soc.* **2001**, *123*, 9338.
- (18) Guthrie, J. P. *Can. J. Chem.* **1978**, *56*, 2342.
- (19) Bethell, D.; Fessey, R.; Namwindwa, E.; Roberts, D. *J. Chem. Soc. Perkin Trans. 2* **2001**, 1489.
- (20) (a) Ando, T.; Yamatake, H.; Morisaki, H.; Yamawaki, J.; Kuramochi, J.; Yukawa, Y. *J. Am. Chem. Soc.* **1981**, *103*, 430. (b) Rhodes, Y.; Takino, T. *J. Am. Chem. Soc.* **1970**, *92*, 5270.
- (21) Lad, C.; Williams, N.; Wolfenden, R. *Proc. Natl. Acad. Sci. U.S.A.* **2003**, *100*, 5607.
- (22) Schroeder, G.; Lad, C.; Wyman, P.; Williams, N.; Wolfenden, R. *Proc. Natl. Acad. Sci. U.S.A.* **2006**, *103*, 4052.
- (23) It bears noting that the relative nucleofugacity of SO_4^{2-} appears to be intermediate between that of the $\text{O}-\text{P}(\text{O})(\text{OCH}_3)_2$ and $\text{CH}_3\text{O}-\text{PO}_3^{2-}$ groups as judged by the rates of methyl transfer to water via C–O bond cleavage at 25 °C. Wolfenden, R.; Ridgway, C.; Young, G. *J. Am. Chem. Soc.* **1998**, *120*, 833. Aksnes, G.; Bergesen, K. *Acta Chem. Scand.* **1966**, *30*, 2508.
- (24) Rate data for hydrolysis of **2a** and **2c** at 25 °C were available directly.
- (25) A plot of ΔH^\ddagger versus $\text{p}K_a^{\text{LG}}$ fits the linear equation $\Delta H^\ddagger = (2.64 \pm 0.24) \text{p}K_a^{\text{LG}} + (5.9 \pm 1.9)$, $r^2 = 0.9456$ (9 data).
- (26) A less extensive Brønsted plot of $\log(k_{25}) = (-1.75 \pm 0.07) \text{p}K_a^{\text{LG}} + (2.7 \pm 0.4)$ can be constructed from the rate data for substrates **2a**, **2c**, and **2d** not involving the long temperature extrapolations required for the other substrates (Figure S10, Supporting Information).
- (27) Hopkins, A.; Day, R.; Williams, A. *J. Am. Chem. Soc.* **1983**, *105*, 6062.
- (28) Matts, P.; White, G.; Payne, W. *Biochem. J.* **1994**, *304*, 937.
- (29) The equilibrium $\text{ROSO}_3^- + \text{OH}^- \rightleftharpoons \text{RO}^- + \text{HOSO}_3^-$ is described by the equation $\log(K) = -1.74\text{p}K_a^{\text{ROH}} + 28.71$ at 25 °C and as originally pointed out by Williams obtains for both aryl and alkyl sulfate monoesters.²⁷ It seems reasonable that the kinetic relationship of $\log(k_{25}^{\text{N}}) = (-1.81 \pm 0.09) \text{p}K_a^{\text{LG}} + (3.6 \pm 0.7)$ determined here will also apply to both alkyl and aryl sulfates considering the similar formal charges born by the leaving group at the transition and product states.
- (30) Crescenzi, A.; Dodgson, K.; White, G. *Biochem. J.* **1984**, *223*, 487.
- (31) Silva, A.; Kong, X.; Hider, R. *Biometals* **2009**, *22*, 771.
- (32) Olguin, L.; Askew, S.; O'Donoghue, A.; Hollfelder, F. *J. Am. Chem. Soc.* **2008**, *130*, 16547.
- (33) (a) Cloves, J.; Dodgson, K.; Games, D.; Shaw, D.; White, G. *Biochem. J.* **1977**, *167*, 843. (b) Cloves, J.; Dodgson, K.; White, G.; Fitzgerald, J. *Biochem. J.* **1980**, *185*, 23.
- (34) Holtz, K. M.; Kantrowitz, E. R. *FEBS Lett.* **1999**, *462*, 7.
- (35) (a) Lukatela, G.; Krauss, N.; Theis, K.; Selmer, T.; Gieselmann, V.; von Figura, K.; Saenger, W. *Biochemistry* **1998**, *37*, 3654. (b) Recksiek, R.; Selmer, T.; Dierks, T.; Schmidt, B.; von Figura, K. *J. Biol. Chem.* **1998**, *273*, 6096. (c) Chai, C. L. L.; Loughlin, W. A.; Lowe, G. *Biochem. J.* **1992**, *287*, 805.
- (36) Kirby, A. J.; Vargolis, A. G. *J. Am. Chem. Soc.* **1967**, *89*, 415.
- (37) In ref 22, a rate constant of $5 \times 10^{-19} \text{ s}^{-1}$ was estimated for hydrolysis of an alkyl phosphate monoester dianion with a leaving group $\text{p}K_a^{\text{LG}}$ of 15.5 at 39 °C. We have made the rate comparison here between a phosphate and sulfate monoester using *n*-pentyl oxide as the leaving group with $\text{p}K_a^{\text{LG}}$ of 16.1.
- (38) Rate data the hydrolysis of aryl phosphate monoester dianions taken from refs 22 and 36.